J|A|C|S
ARTICLES
Published on Web 11/04/2006

^{15}N Solid-State NMR Provides a Sensitive Probe of Oxidized Flavin Reactive Sites

Ronald L. Koder, Jr.,[†,‡,1] Joseph D. Walsh,[†,2] Maxim S. Pometun,[§,3] P. Leslie Dutton,[‡] Richard J. Wittebort,[§] and Anne-Frances Miller*[,†]

Contribution from the Department of Chemistry, University of Kentucky, Lexington, Kentucky 40506-0055, Department of Biochemistry and Biophysics, The Johnson Research Foundation, University of Pennsylvania, Philadelphia, Pennsylvania 19104, and Department of Chemistry, University of Louisville, Louisville, Kentucky 40292

Received July 9, 2006; E-mail: afm@uky.edu

Abstract: Flavins are central to the reactivity of a wide variety of enzymes and electron transport proteins. There is great interest in understanding the basis for the different reactivities displayed by flavins in different protein contexts. We propose solid-state nuclear magnetic resonance (SS−NMR) as a tool for directly observing reactive positions of the flavin ring and thereby obtaining information on their frontier orbitals. We now report the SS−NMR signals of the redox-active nitrogens N1 and N5, as well as that of N3. The chemical shift tensor of N5 is over 720 ppm wide, in accordance with the predictions of theory and our calculations. The signal of N3 can be distinguished on the basis of coupling to ^{1}H absent for N1 and N5, as well as the shift tensor span of only 170 ppm, consistent with N3's lower aromaticity and lack of a nonbonding lone pair. The isotropic shifts and spans of N5 and N1 reflect two opposite extremes of the chemical shift range for "pyridine-type" N's, consistent with their electrophilic and nucleophilic chemical reactivities, respectively. Upon flavin reduction, N5's chemical shift tensor contracts dramatically to a span of less than 110 ppm, and the isotropic chemical shift changes by approximately 300 ppm. Both are consistent with loss of N5's nonbonding lone pair and decreased aromaticity, and illustrate the responsiveness of the ^{15}N chemical shift principal values to electronic structure. Thus. ^{15}N chemical shift principal values promise to be valuable tools for understanding electronic differences that underlie variations in flavin reactivity, as well as the reactivities of other heterocyclic cofactors.

Introduction

Heterocycles feature strongly among reactive biological molecules. Their heteroatoms make crucial contributions to the reactivity of many enzyme cofactors, including pterins, flavins, pyridoxyl phosphate, and more. They also mediate the H-bonding that underlies the stable but reversible associations so critical to life, in the guise of DNA base pairing and protein structure. Thus, understanding the interactions and the consequences of these functionalities is a very important element of understanding biological chemistry and biomolecular function.

7,8-Dimethyl-10-alkylisoalloxazines, called flavins (Figure 1), possess remarkable chemical versatility.[4] The flavin component of the cofactors FMN and FAD[5] is used throughout biological chemistry to execute reactions ranging from oxygenation, oxidation and reduction, disulfide formation and rereduction, and dehydrogenation.[6,7] The central diazabutadiene motif is able to accommodate two electrons and two protons, either sequentially or in combinations, via effective redefinition of the N1 and N5 frontier orbitals.

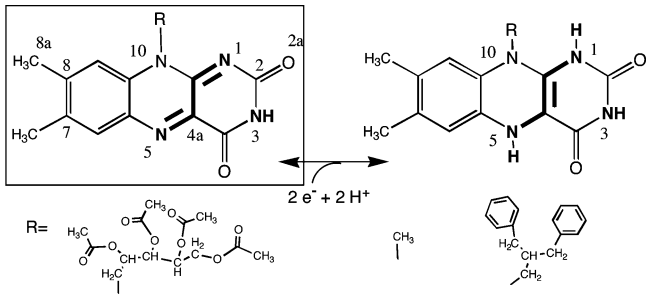

Figure 1. Structure of oxidized flavin, boxed, with the effect of two-electron reduction, numbering of the N positions, and side chains of the flavin variants used in this work. The flavin's diazabutadiene motif is in bold, R = tetraacetyl ribityl (bottom left) for TARF, R = methyl (bottom center) for lumiflavin, and R = dibenzyl ethyl (bottom right) for dBF.

[†] University of Kentucky.
[‡] University of Pennsylvania.
[§] University of Louisville.
(1) Current address: Department of Physics, The City College of New York, New York, NY 10031.
(2) Current address: Department Structural Biology, University of Pittsburgh School of Medicine, Pittsburgh, PA 15260.
(3) Current address: Department of Biochemistry and Biophysics, The Johnson Research Foundation, University of Pennsylvania, Philadelphia, PA 19104.
(4) Massey, V. *Biochem. Soc. Trans.* **2000**, *28*, (4), 283−296.
(5) Abbreviations: CP, cross-polarization; dBF, dibenzyl flavin; DFT, density functional theory; FAD, flavin adenine dinucleotide; FMN, flavin mononucleotide; GIAO, gauge-including atomic orbital; HOMO, highest occupied molecular orbital, used somewhat loosely here to include the several such orbitals that define the reactivity; LUMO, lowest unoccupied molecular orbital, used somewhat loosely to include the several lowest-lying orbitals that define the reactivity; MAS, magic angle spinning; NMR, nuclear magnetic resonance; PASS, phase adjusted spinning sideband; rmsd, root-mean-square deviation; SS, solid state; TARF, tetraacetyl riboflavin.

10.1021/ja0648817 CCC: $33.50

Nature's widespread use of cofactors with broad chemical capability makes evolutionary sense, as this strategy minimizes the number of different cofactors which must be elaborated. However, for a given enzyme to display only a particular reactivity, the protein must then be able to tune and constrain the reactivity of bound cofactors. Proteins use a variety of devices to modulate the reactivity of bound flavins.[8−15] In part, this is achieved by virtue of the fact that the delocalized frontier orbitals of flavins encompass several O and N functionalities whose geometry, H-bonding, and protonation status may be expected to strongly modulate the energy and distribution of HOMO electron density.[16−20] Thus, the energies and natures of the flavin frontier orbitals are proposed to vary from enzyme to enzyme, in a manner that correlates with the reactivity.[20−23] Indeed, the optical, fluorescence, and Stark spectra of FMN and FAD vary significantly depending on the protein site in which the latter are bound.[24,25] However, it is sometimes difficult to relate such spectral differences to specific atoms or orbitals, and the interpretation of the spectral differences may not be unique. Flavin vibrational frequencies can be interpreted in terms of more local effects,[26−28] but possibly the most site-specific probes available so far are EPR hyperfine couplings for the semiquinone states[29] and NMR chemical shifts for the diamagnetic states.[30−33]

NMR chemical shifts and J-couplings have been interpreted in elegant detail in terms of π electron density, sp^2/sp^3 character and hydrogen bonding at various sites, leading to valuable insights into the polarization of the flavin ring system, its protonation state, hydrogen bonding, and pyramidalization at N10 and N5.[30−32,34,35] However, the isotropic shifts measured in solution represent the average of all the effects on total electron density. Yet, many interactions involve specific orbitals, and certain orbitals are much more important than others in shaping flavin chemistry. One would like to obtain information that emphasizes those.

Solid-state NMR (SS−NMR) can reveal all the elements of the chemical shift tensor for single-crystal samples[36] or measure principal values and the corresponding eigenvectors' orientations relative to another vector in the molecular frame, such as a dipole−dipole vector.[37−39] Even for powder or polycrystalline samples, SS−NMR yields all three chemical shift principal values (CSPVs) separately. Experiments have shown that the different CSPVs often reflect different properties, such as protonation state vs hydrogen bonding status, for carboxyl carbons[40] and imidazole ring nitrogens.[41] This is consistent with the origins of the paramagnetic contribution to chemical shift, whose different PVs are in theory related to different HOMO and LUMO combinations.

Ramsey's equation (eq 1)[42] predicts that NMR chemical shifts (δ) will reflect shielding due to ground-state electron density (the so-called diamagnetic contribution, $\sigma_{ii,d}$), as well as deshielding due to electron orbital angular momentum ($\sigma_{ii,p}$).[43]

$$-\delta_{ii} = \sigma_{ii} = \sigma_{ii,d} - \sigma_{ii,p} \tag{1a}$$

$$\sigma_{ii,d} = \frac{e^2}{2m_e c^2}\left\langle 0\left|\frac{j^2 + k^2}{r^3}\right|0\right\rangle \tag{1b}$$

$$\sigma_{ii,p} \approx \left(\frac{e\bar{h}}{2m_e c}\right)^2 \Sigma_n \left(\frac{\langle 0|\hat{L}i|n\rangle \left\langle n\left|\frac{2\hat{L}i}{r^3}\right|0\right\rangle}{E_n - E_0} + \frac{\left\langle 0\left|\frac{2\hat{L}i}{r^3}\right|n\right\rangle \langle n|\hat{L}i|0\rangle}{E_n - E_0} \right) \tag{1c}$$

The paramagnetic shielding is thus expected to be particularly sensitive to the natures and relative energies of the frontier orbitals, as the different PVs, $\sigma_{ii,p}$, reflect different ground state ($\langle 0|$) and excited state ($|n\rangle$) combinations coupled by different components of orbital angular momentum ($\hat{L}i$) and separated by different energies ($\Delta E = E_n - E_0$).[42,44]

(6) Massey, V. *FASEB J.* **1995**, *9*, 473−475.
(7) Walsh, C. *Enzymatic Reaction Mechanisms*; W. H. Freeman: New York, 1979.
(8) Cuello, A. O.; McIntosh, C. M.; Rotello, V. M. *J. Am. Chem. Soc.* **2000**, *122*, 3517−3521.
(9) Yin, Y.; Sampson, N. S.; Vrielink, A.; Lario, P. I. *Biochemistry* **2001**, *40*, 13779−13787.
(10) Hasford, J. J.; Rizzo, C. J. *J. Am. Chem. Soc.* **1998**, *120*, 2251−2255.
(11) Zhou, Z.; Swenson, R. P. *Biochemistry* **1996**, *35*, 15980−15988.
(12) Guo, F.; Chang, B. H.; Rizzo, C. J. *Bioorg. Med. Chem. Lett.* **2002**, *12*, 151−154.
(13) Akiyama, T.; Simeno, F.; Murakami, M.; Yoneda, F. *J. Am. Chem. Soc.* **1992**, *114*, 6613−6620.
(14) Talfournier, F.; Munro, A. W.; Basran, J.; Sutcliffe, M. J.; Daff, S.; Chapman, S. K.; Scrutton, N. S. *J. Biol. Chem.* **2001**, *276* (23), 20190−20196.
(15) Ludwig, M. L.; Pattridge, K. A.; Metzger, A. L.; Dixon, M. M.; Eren, M.; Feng, Y.; Swenson, R. P. *Biochemistry* **1997**, *36*, 1259−1280.
(16) Nishimoto, K.; Fukunaga, H.; Yagi, K. *J. Biochem. (Tokyo)* **1986**, *100*, 1647−1653.
(17) Yalloway, G. N.; Löhr, F.; Rüterjans, H. In *Flavins and Flavoproteins*; Chapman, S., Perham, R., Scrutton, N. S., Eds.; Rudolf Weber: University of Cambridge, UK, 2002; pp 679−684.
(18) Hasford, J. J.; Kemnitzer, W.; Rizzo, C. J. *J. Org. Chem.* **1997**, *62* (16), 5244−5245.
(19) Walsh, J. D.; Miller, A.-F. *J. Phys. Chem. B* **2003**, *107*, 854−863.
(20) Niemz, A.; Rotello, V. M. *Acc. Chem. Res.* **1999**, *32*, 44−52.
(21) Massey, V.; Hemmerich, P. *Biochem. Soc. Trans.* **1980**, *8*, 246−257.
(22) Müller, F.; Walker, W. H.; Massey, V.; Brustlei, M.; Hemmerich, P. *Eur. J. Biochem.* **1972**, *25* (3), 573.
(23) Massey, V.; Ghisla, S.; Moore, E. G. *J. Biol. Chem.* **1979**, *254* (19), 9640−9650.
(24) Sikorska, E.; Khmelinskii, I.; Koput, J.; Bourdelande, J. L.; Sikorski, M. *J. Mol. Str.* **2004**, *697* (1−3), 137−141.
(25) Hopkins, N.; Stanley, R. J. *Biochemistry* **2003**, *42* (4), 991−999.
(26) Schelvis, J. P. M.; Ramsey, M.; Sokolova, O.; Tavares, C.; Cecala, C.; K., C.; Wagner, S.; Gindt, Y. M. *J. Phys. Chem. B* **2003**, *107* (44), 12352−12362.
(27) Wille, G.; Ritter, M.; Friedemann, R.; Mantele, W.; Hubner, G. *Biochemistry* **2003**, *42* (50), 14814−14821.
(28) Zheng, Y. G.; Carey, P. R.; Palfey, B. A. *H. Raman Spec.* **2005**, *35* (7), 521−525.
(29) Weber, S.; Möbius, K.; Richter, G.; Kay, C. W. M. *J. Am. Chem. Soc.* **2001**, *123*, 3790−3798.
(30) Müller, F. In *Chemistry and Biochemistry of Flavoenzymes*; Müller, F., Ed.; CRC: Boca Raton FL, 1992; Vol. III, pp 558−595.
(31) Eisenreich, W.; Kemter, K.; Bacher, A.; Mulrooney, S. B.; Williams, C. h.; Müller, F. *Eur. J. Biochem.* **2004**, *271* (8), 1437−1452.
(32) Moonen, C. T. W.; Vervoort, J.; Müller, F. *Biochemistry* **1984**, *23*, 4859−4867.
(33) Rüterjans, H.; Fleischmann, G.; Löhr, M.; Knauf, F.; Blümel, M.; Lederer, F.; Mayhew, S. G.; Müller, F. *Biochem. Soc. Trans.* **1996**, *24*, 116−121.
(34) Yagi, K.; Ohishi, N.; Takai, A.; Kawano, K.; Kyogoku, Y. *Biochem. (Tokyo)* **1976**, *15* (13), 2877−2880.
(35) Vervoort, J.; Müller, F.; Mayhew, S. G.; van den Berg, W. A. M.; Moonen, C. T. W.; Bacher, A. *Biochemistry* **1986**, *25*, 6789−6799.
(36) Waddell, K. W.; Chekmenev, E.; Wittebort, R. J. *J. Am. Chem. Soc.* **2005**, *127*, 9030−9035.
(37) Oas, T. G.; Hartzell, C. J.; Dahlquist, F. W.; Drobny, G. P. *J. Am. Chem. Soc.* **1987**, *109*, 5962−5966.
(38) Hartzell, C. J.; Whitfield, M.; Oas, T. G.; Drobny, G. P. *J. Am. Chem. Soc.* **1987**, *109*, 5966−5969.
(39) Munovitz, M.; Aue, W. P.; Griffin, R. G. *J. Chem. Phys.* **1982**, *77*, 1686−1689.
(40) Gu, Z.; Zambrano, R.; McDermott, A. *J. Am. Chem. Soc.* **1994**, *116*, 6368−6372.
(41) Wei, Y.; de Dios, A. C.; McDermott, A. E. *J. Am. Chem. Soc.* **1999**, *121*, 10389−10394.
(42) Ramsey, N. F. *Phys. Rev.* **1950**, *78* (6), 699−703.
(43) $\sigma_{ii,p}$ is called the paramagnetic contribution because it augments the applied field, not because of any relationship with unpaired electrons.
(44) Drago, R. S. *Physical Methods for Chemists*; Saunders College Publishing: New York, 1992.

Paramagnetic deshielding tends to be dominated by contributions from the orbital coupling of HOMOs to LUMOs, because these terms are scaled by the inverse of the smallest energy gap (eq 1c). Moreover, the HOMOS and the LUMOS are precisely the orbitals that dominate the chemistry, so these chemical shifts should be related to reactivity. The effect is particularly significant for atoms in conjugated systems, especially sites with a nonbonded lone pair, because lower energy gaps will apply, so these sites are predicted to display particularly large paramagnetic deshielding and correspondingly large chemical shifts.

The three CSPVs each reflect HOMOs and LUMOs that are perpendicular to each other and also perpendicular to the shielding component in question (see supplemental Figure 1, Supporting Information).[42,45] Thus, each PV can reflect different HOMO and LUMO combinations, and the large deshielding due to a nonbonded lone pair tends to be concentrated in one PV.[46] For N1 and N5 of oxidized flavins, this one value is calculated to change almost three times as much as the isotropic shift, in response to hydrogen bonding such as is often observed in proteins.[19] Thus, SS−NMR should provide great sensitivity to noncovalent interactions that tune flavin reactivity. In summary, paramagnetic deshielding tends to emphasize precisely the orbitals involved in cofactor reactivity, it is large in conjugated systems especially at N sites, and individual PVs can often be related to specific orbitals. Thus, ^{15}N SS−NMR is uniquely well suited to understanding the electronic basis for flavin reactivity and its modulation by proteins.

These predictions for flavins are supported by studies of other systems. In extensive SS NMR observations of ^{15}N in heterocycles and in H-bonds, Grant, Wasylishen and others have demonstrated key predictions of Ramsey's equation.[42] The most strongly deshielded CSPV is indeed the one whose eigenvector is perpendicular to the plane described by the occupied and unoccupied orbitals separated by the smallest energy gap.[46,47] This CSPV is also extremely sensitive to electronic perturbation both via substitution at positions that participate in the conjugated orbital system[46] and via noncovalent interactions, including H bonding.[19,47−50] The results are consistent with Ramsey's prediction that interactions that stabilize the lone pair and increase the corresponding energy gap, ΔE, will decrease the deshielding that reflects the lone pair, in particular.[42,44,47,51] Similarly, individual PVs of the ^{15}N chemical shift tensor were found to correlate with the electronegativity of para-substituents of nitrobenzene even when the isotropic shift did not.[52] Thus, there is ample evidence that the different PVs of the ^{15}N chemical shift tensor respond in different ways and often with different signs, to perturbations typical of interactions between biomolecules[19,47,49] and perturbations of the frontier orbitals that are also associated with altered reactivity. Nonetheless, only isotropic ^{15}N or ^{13}C chemical shift information has been made available for flavins thus far.

We now report the first study of SS−^{15}N NMR signals of flavins [53,54] and demonstrate that these adhere well to the predictions of theory and that their properties discriminate between the different labeled nitrogens. The chemical shift principle values of the N sites in oxidized flavin are clearly distinct from one another, spanning up to 724 ppm for the N5 site, and distinguishing between chemically different N sites in the flavin even when these appear to have similar local bonding environments. Most of the ^{13}C resonances occur in bunches and are not sufficiently distinct to permit assignment without selective labeling, but their CSPVs can be accounted for by our calculated values. Three ^{15}N signals, however, have been assigned experimentally, and the CSPVs obtained for them display an rms deviation from calculated values of 19 ppm. The CSPVs thus validate our calculations of flavin electronics, which therefore can in turn be used to understand the different CSPVs and the flavin electronics. Extension of this approach should allow us to understand the different *reactivities* of different sites, and different flavins, in conjunction with SS−NMR observations of flavin N's, and C's.

Experimental Methods

Synthesis. Initial studies have used [^{15}N−N1, N3, N5]-TARF as a proof of principle. Labeled riboflavins were synthesized by the method of Lambooy,[55] substituting cyanoborohydride reduction of the imine intermediate for the original catalytic hydrogenation. Labels were introduced using ^{15}N $NaNO_2$ for N5 and ^{15}N urea (Cambridge Isotope Labs) for N1 and N3. Labeled riboflavins were tetra-acetylated using acetic anhydride in pyridine. N(10)−(2,2-dibenzylethyl) isoalloxazine (dBF) labeled at the N5 position was synthesized following a modification of the method of Tishler.[56] Details are to be published elsewhere. dBF provides the advantage of being soluble in nonpolar medium and thus of being readily separable from the dithionite salt solution used to prepare chemically reduced flavin (below).

Reduction of dBF. Working under inert atmosphere, dBF was dissolved in degassed ethyl acetate and shaken with a 2-fold larger volume of sodium dithionite in degassed aqueous 100 mM KOH (20-fold stoichiometric excess of dithionite over dBF). No color was seen to migrate into the aqueous phase. The aqueous phase was removed, and the organic phase was dried under a stream of Ar, before being packed into an NMR rotor, under inert atmosphere. The rotor (which was not airtight) was transferred quickly into the NMR probe under a stream of N_2 and maintained under an N_2 atmosphere for observation. Following observation of the reduced state signal, the N_2 stream was replaced with a flow of air (also used for maintaining NMR probe temperature and sample spinning). Within 12 h, the reduced state signal had disappeared and was replaced by that of the oxidized state.

NMR Conditions. ^{15}N spectra were collected at 40 MHz for ^{15}N with signal enhancement via ramped cross polarization from ^{1}H, and TPPM2 decoupling during acquisition.[57] Details are given in each figure caption. Pulse sequences were those provided by Varian Inc. Lower

(45) Mason, J. In *Encyclopedia of NMR*; Grant, D. M., Harris, R. K., Eds.; Wiley: Sussex UK, 1996; pp 3222−3251.
(46) Lumsden, M. D.; Wu, G.; Wasylishen, R. E.; Curtis, R. D. *J. Am. Chem. Soc.* **1993**, *115* (7), 2825−2832.
(47) Solum, M. S.; Altmann, K. L.; Strohmeier, M.; Berges, D. A.; Zhang, Y.; Facelli, J. C.; Pugmire, R. J.; Grant, D. M. *J. Am. Chem. Soc.* **1997**, *119*, 9804−9809.
(48) Facelli, J. C.; Pugmire, R. J.; Grant, D. M. *J. Am. Chem. Soc.* **1996**, *118*, 5488−5489.
(49) Stueber, D.; Grant, D. M. *J. Am. Chem. Soc.* **2002**, *124*, 10539−10551.
(50) Harbison, G. S.; Herzfeld, J.; Griffin, R. G. *Biochemistry* **1983**, *22* (1), 1−5.
(51) Duthaler, R. O.; Roberts, J. D. *J. Am. Chem. Soc.* **1978**, *100* (16), 4969−4973.
(52) Penner, G. H.; Bernard, G. M.; Wasylishen, R. E.; Barrett, A.; Curtis, R. D. *J. O. C.* **2003**, *68*, 4258−4264.
(53) A preliminary spectrum was included in a conference proceedings. See Miller, A.-F.; Koder, R. L., Jr.; Walsh, J. D.; Zhang, P.; Haynes, C. A.; Rodgers, D. W. In *Flavins and Flavoproteins*; Nishino, T., Ed.; Small World Press: Japan, 2005; Vol. 15, pp 261−269.
(54) Miller, A.-F.; Koder, R. L., Jr.; Walsh, J. D.; Zhang, P.; Haynes, C. A.; Rodgers, D. W. In *Flavins and Flavoproteins*; Nishino, T., Ed.; Small World Press: Japan, 2005.
(55) Lambooy, J. P. *Methods Enzymol.* **1971**, *18b*, 437−447.
(56) Tishler, M.; Pfister, K., 3rd; Babson, R. D.; Ladenburg, K.; Fleming, A. J. *J. Am. Chem. Soc.* **1947**, *69*, 1487−1492.
(57) Bennett, A. E.; Rienstra, C. M.; Auger, M.; Lakshmi, K. V.; Griffin, R. G. *J. Chem. Phys.* **1995**, *103* (16), 6951−6958.

temperatures and higher cross-polarization fields were found to increase the ^{15}N signal-to-noise by a factor of up to two without altering signal shapes or intensity distributions. However, the lowest accessible temperatures proved not to be stable on some days, and higher cross-polarization powers than 50 kHz proved not to be advisable for the instrumentation, requiring compromise for longer runs. Room temperature was used for the reduction and reoxidation experiment (Figure 9) in order to be able to use air to reoxidize the sample in situ. Thus, air was used as the temperature control and spinning drive gas in this case, and long interscan delays of 60 s were used to minimize possible sample heating. ^{13}C spectra were collected at room temperature with interscan delays of 5 s., contact times of 8 ms at a cross-polarization field of 50 kHz for ^{1}H and ^{1}H TPPM2 decoupling at 55 kHz. Spinning speeds of 2250 and 4000 Hz were used for the 2d-PASS spectra used to determine ^{13}C CSPVs. All ^{15}N chemical shifts are quoted relative to liquid ammonia, and spectra were referenced indirectly against the ^{15}N signals of NH_4NO_3 at 21 and 376 ppm, respectively.[58] ^{13}C chemical shifts are quoted relative to TMS at 0 ppm and calibrated indirectly against hexamethyl benzene (17.3 ppm).

Calculations. GIAO calculations of NMR shielding tensors[59,60] were performed as described in detail by Walsh and Miller[19] using 7,8,10-trimethylisoalloxazine (lumiflavin, Figure 1), to concentrate computational effort on the flavin ring system rather than the side chain. The G6−311(d,p) basis and B3PW91 functional[61] were used because they yielded the best agreement with experimental oxidized state flavin structures and isotropic chemical shifts measured in $CDCl_3$,[32] with performance comparable to those of larger basis sets including cc-pVTZ.[19] The use of DFT methods in both geometry optimization and chemical shift calculation was found to be essential, consistent with the importance of electron correlation expected for the highly conjugated frontier orbitals of oxidized flavins[19] (also see Barfield[62]). All calculations were performed using the Gaussian 98 or Gaussian 03 package[63] on the University of Kentucky's N- and X-class HP supercomputers. Calculated ^{15}N shieldings were converted to calculated chemical shifts by subtracting the former from the shielding of liquid ammonia of 244.6 ppm (264.5 ppm plus the gas to liquid correction).[64] Calculated ^{13}C shieldings were converted to calculated chemical shifts by subtracting the former from the shielding of liquid TMS of 186.4 ppm.[19] According to convention, the PVs are numbered in order of magnitude, with δ_{11} being the most deshielded one (highest chemical shift value) and δ_{33} the most shielded. Figure 8 was generated using molscript.[65]

Results and Discussion

Observation of Reactive N Sites in the Flavin Ring: A Single Signal Spans Over 700 ppm. Figure 2A shows the two-dimensional phase adjusted spinning sideband spectrum (PASS)[66,67] of tetraacetyl riboflavin (TARF) labeled with ^{15}N at positions N1, N3 and N5 [68] (see Figure 1). The corresponding one-dimensional cross-polarized magic angle spinning (CP-MAS) spectrum is shown above (2B). The central row of the

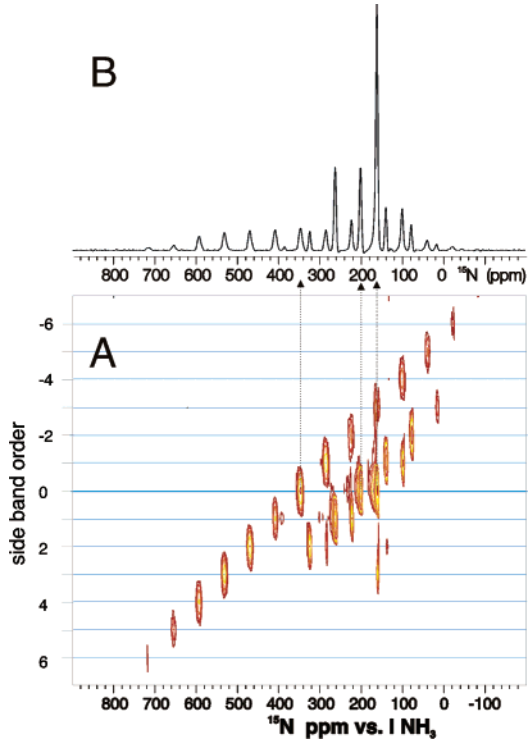

Figure 2. ^{15}N 2d-PASS spectrum[66,67] of oxidized [^{15}N−N1,N3,N5]-TARF spinning at 2.5 kHz (A), compared with a 1d CP-MAS spectrum of the same sample (B) also spinning at 2.5 kHz. Vertical arrows indicate the positions of the isotropic shifts in the two spectra. 50 kHz CP for ^{1}H and 45 kHz ramped CP for ^{15}N were applied for 15 ms, at −60 °C, with 5 s between scans. ^{1}H was excited with a 5.4 μs 90° pulse and decoupled at 51 kHz over the 20 ms acquisition time.

PASS spectrum isolates the isotropic shifts of each labeled N (vertical arrows), although these are difficult to identify in the 1d CP-MAS spectrum. The isotropic shifts are within 5 ppm of the isotropic average shifts observed for TARF in solution in $CDCl_3$[30] (Table 1). The other rows of the PASS spectrum each contain one spinning sideband from each signal, over the spectral width spanned by each of the signals.[66] Thus, the three sets of spinning sidebands can readily be identified as diagonal arrays[69] although they overlap significantly in the 1d CP-MAS spectrum.

Assignment of the Signals to Each of N1, N3, and N5. The signal of N5 was identified by comparison of the CP-MAS spectrum of [^{15}N−N1,N3,N5]-TARF with that of dibenzyl flavin (dBF) labeled exclusively at N5 (Figure 3). Thus, we find that the signal of TARF N5 has an isotropic shift of 345 ppm and spans over 700 ppm.

Of the N's, only N3 has a directly bonded ^{1}H (Figure 1). This property could be detected indirectly based on the strong line broadening experienced by the N3 signal, but not those of N1 or N5, when the ^{15}N spectrum was collected without use of ^{1}H decoupling (Figure 4), consistent with N3's 10-fold higher ^{1}H-^{15}N nOe in solution.[34] Thus, we assign the isotropic shift of 159 ppm and associated sidebands to N3. The remaining signal is therefore attributed to N1, with an isotropic shift of 199 ppm and a span of approximately 300 ppm.

These assignments were confirmed experimentally by the very different rate of cross-polarization of N3 vs the very similar

(58) Duncan, T. M. *Chemical Shift Tensors*, 2nd ed.; Farragut Press: Madison, WI, 1997.
(59) Cheeseman, J. R.; Trucks, G. W.; Keith, T. A.; Frisch, M. J. *J. Chem. Phys.* **1996**, *104* (14), 5497−5509.
(60) Ditchfield, R. J. *J. Chem. Phys.* **1972**, *56*, 5688−5691.
(61) Perdew, J. P.; Wang, Y. *Phys. Rev. B* **1992**, *45*, 13244−13249.
(62) Barfield, M.; Fagerness, P. *J. Am. Chem. Soc.* **1997**, *119*, 8699−8711.
(63) Frisch, M. J.; et al. *Gaussian 98, Revision A.7*. Gaussian Inc.: Pittsburgh, PA, 1998.
(64) Jameson, C. J.; Jameson, A. K.; Oppusunggu, D.; Wille, S.; Burrell, P. M.; Mason, J. *15N nuclear magnetic shielding scale from gas-phase studies* **1981**, *74*, 81−88.
(65) Kraulis, P. J. *J. Appl. Crystallogr.* **1991**, *24*, 946−950.
(66) Antzutkin, O. N.; Lee, Y. K.; Levitt, M. H. *J. Magn. Reson.* **1998**, *135* (1), 144−155.
(67) Antzutkin, O. N.; Shekar, S. C.; Levitt, M. H. *J. Magn. Reson. A* **1995**, *115*, 7−19.
(68) N10 is also interesting but is more expensive to label and so will be addressed in future studies.
(69) Spinning sidebands occur at intervals equal to the spinning speed on each side of the isotropic shift, over the spectral width of the signal.

Table 1. Oxidized State Chemical Shift Principal Values[a]: **Experimental** (and Calculated), Compared with *Isotropic Values for TARF in $CDCl_3$*

	δ_{11} CP-MAS, PASS	δ_{22} CP-MAS, PASS	δ_{33} CP-MAS, PASS	$\delta_{iso} = (\delta_{11}+\delta_{22}+\delta_{33})/3$	span = δ_{11}-δ_{33}
N1	**319, 332** (328[b])	**252, 241** (241)	**26, 24** (30)	**199, 199** (200[b]) *200*	**293, 307** (297)
N3	**272, 233** (237)	**104, 147** (134)	**98, 98** $(117)_s$	**158, 159** (163) *160*	**174, 135** (120)
N5	**684, 688** (699[b])	**392, 379** $(396)_s$	**−40, −33** (−33)	**345, 345** (354[b]) *346*	**724, 722** (731)
N10	(222)	(152)	(59)	(144) *152*	(163)

[a] Chemical shift relative to liquid ammonia. Experimental values were obtained both from 1d CP-MAS spectra collected at a range of MAS speeds (2.5 kHz − 5 kHz) and from 2d-PASS spectra collected at MAS speeds of 2.5 kHz and 5 kHz. Uncertainties associated with PVs are estimated at 11 ppm based on comparison of values obtained from separate experimental determinations at a range of MAS speeds. The δ_{33} PV of N3 is less well determined than the other values (± 25 ppm), likely because this signal is narrow and would have benefitted from measurements at slower spinning speeds than our instrument permits. [b] For N1 and N5, a gas-phase to condensed-phase correction of −12 ppm is applied to the calculated isotropic shift, based on data for pyridine,[51,78] and the corresponding maximum correction to δ_{11} of −36 ppm is also incorporated (see text).

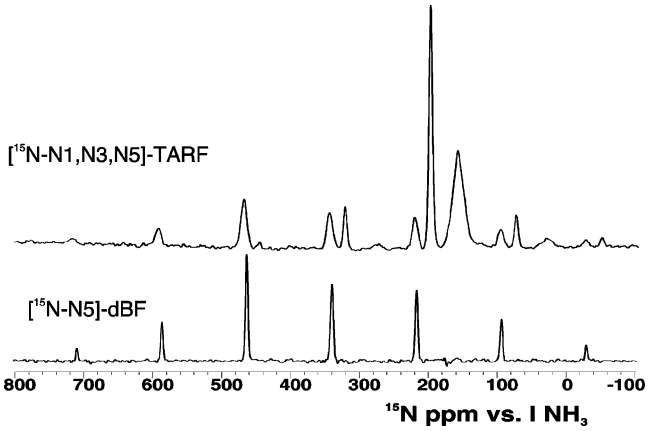

Figure 3. Comparison of the ^{15}N CP-MAS spectrum of oxidized [^{15}N−N1,N3,N5]-TARF (top) with that of oxidized [^{15}N−N5] dBF (dibenzyl flavin, bottom). 25 kHz ramped CP for 20 ms was used at −80 °C, with 10 ms acquisitions and 10 s between scans.

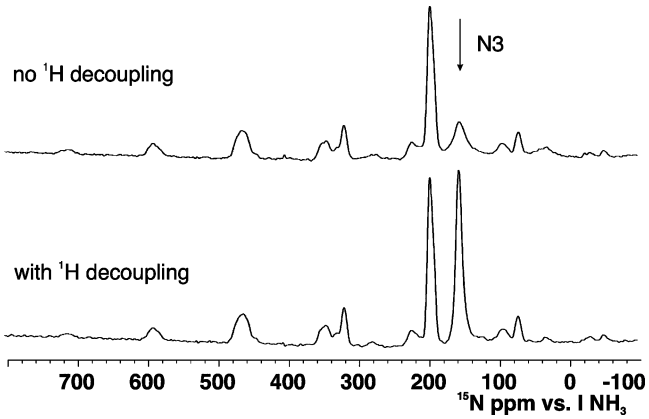

Figure 4. The effect of ^1H decoupling during ^{15}N acquisition, for oxidized [^{15}N−N1,N3,N5]-TARF. 35 kHz ramped CP for 16 ms with MAS at 5 kHz were used at −60 °C, with 10 ms acquisitions and 10 s between scans.

buildups of the signals attributed to N1 and N5 (Figure 5).[70] The rapid buildup of N3 polarization via ^1H-^{15}N cross relaxation corroborates its proximity to a proton. Similarly, N3 is the only N for which decay due to relaxation of the ^1H bath was apparent. In contrast, although N1's isotropic shift and span are very different from those of N5, these two pyridine-type N's nonetheless displayed very similar CP buildup behaviors, which confirms their similar dearth of nearby H's and our assignment of N1.

(70) N3 displays biexponential CP buildup kinetics, consistent with heterogeneity among the sites, or motion affecting N3 and/or its attached H. e.g., see ref 71. The latter possibility is supported by the large improvement in signal intensity obtained at lower temperatures. Similar biexponential buildup in analogous compounds has been reported by Solum et al., ref 47.

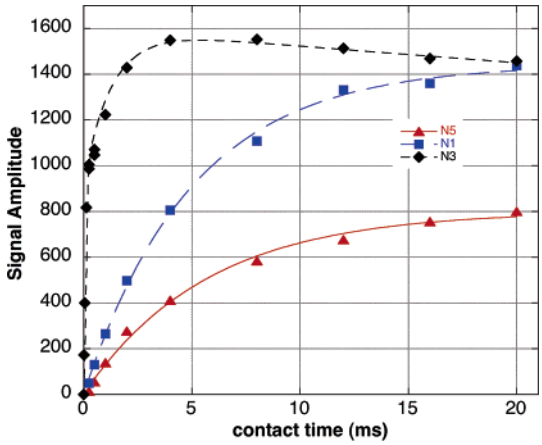

Figure 5. Exponential buildup and decay of ^{15}N signals as a function of CP contact time, for N1 (blue squares), N3 (black diamonds) and N5 (red triangles) of oxidized TARF. CP-MAS spectra were obtained with 5 kHz MAS at − 60 °C with 50 kHz ^1H CP and 45 kHz ramped ^{15}N CP for the time interval specified (*X*-axis). Data were acquired with 51 kHz ^1H decoupling during 20 ms acquisitions, with 10 s delays between scans. Peak intensities were measured for all spinning sidebands. Summed intensities for each signal were fit to Amp*[$1 - \exp(-t/T_{NH})$] for (N1 and N5) or Amp*[$\exp(-t/T_{1\rho H}) - f*\exp(-t/T_{NH,1}) - (1 - f)*\exp(-t/T_{NH,2})$] for N3, where $T_{1\rho H}$ is the rotating frame longitudinal relaxation time of ^1H, T_{NH} is the time constant for $^1H-^{15}N$ cross polarization, Amp denotes the maximum possible signal amplitude, and *f* is the fraction of the population affected by the shorter buildup time $T_{NH,1}$.[71] The curves accompanying the data reflect the following fitted parameter values: for N1, Amp = 1440 ± 20, T_{NH} =5.0 ± 0.2 ms; for N5, Amp = 800 ± 20, T_{NH} = 5.7 ± 0.5 ms; for N3, Amp = 1600 ± 20, two values of T_{NH} are needed to obtain a good fit:[70] T_{NH} = 0.1 ± 0.3 ms for 60% of the population and T_{NH} = 1.3 ± 0.02 ms for 40% of the population, $T_{1\rho H}$ = 200 ± 40 ms.

From a practical standpoint, the slow cross-polarization of N1 and N5 and the fact that N5's signal intensity is distributed among many sidebands, require that NMR conditions be optimized with care. Nonetheless, the above experiments provide experimental assignments for all three signals, and they reveal very different NMR properties related to the bonding and electronic structures of the different N sites. Our experimental assignments permit validation of our calculations without the circular logic implied in making assignments based on agreement with calculated shifts, and then invoking the agreement to validate the calculations.

The Observed Chemical Shift Principal Values Are Well Reproduced by Calculations. The pattern of intensity distribution among the different spinning sidebands yields the three CSPVs of each signal (δ_{11}, δ_{22}, δ_{33}), via Herzfeld-Berger analysis.[72,73] These are reported in Table 1, and agree with

(71) Silvestri, R. L.; Koenig, J. L. *Macromolecules* **1992**, *25*, 2341−2350.
(72) Herzfeld, J.; Berger, R. *J. Chem. Phys.* **1980**, *73* (12), 6021−6032.

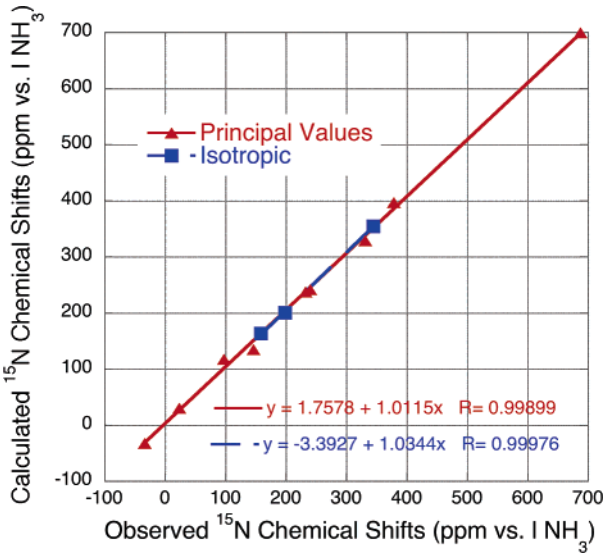

Figure 6. Regression of calculated ^{15}N chemical shifts vs ^{15}N chemical shifts observed for oxidized [^{15}N−N1,N3,N5]-TARF by 2d-PASS at 2.5 kHz MAS. Calculated chemical shifts of N5 and N1 incorporate a correction for solvation effects of −12 ppm to δ_{iso} or −36 ppm to δ_{11}, as described in the text.

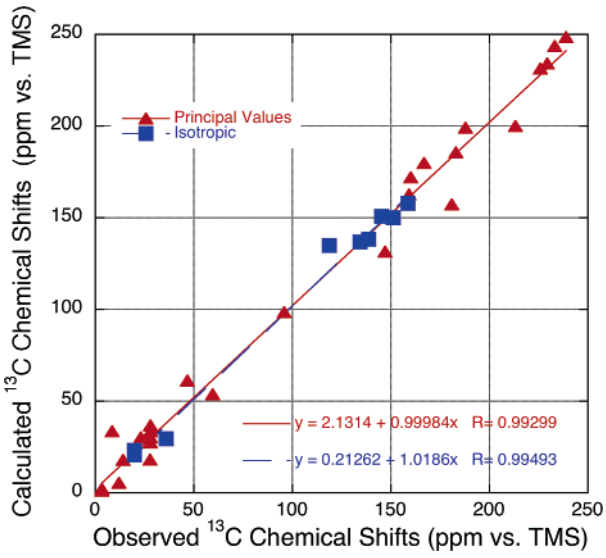

Figure 7. Regression of calculated ^{13}C chemical shifts vs ^{13}C chemical shifts observed for oxidized lumiflavin by PASS at 2.25 kHz MAS. This plot employs the best match between observed signals and calculated signals (each represented by three CSPVs); thus, it should be taken to represent the best possible agreement between the current data set and calculated values.

turning points observed in powder spectra obtained for a static sample. Thus, we find that the observed N5 signal spans over 720 ppm. This is large but not extreme, as pyridine's ^{15}N chemical shift tensor is reported to span 622[47] to 782 ppm.[74,75] The extraordinary spans of 1479 ppm for *p*-nitroso-*N*,*N*-dimethylaniline[46] and 1048 ppm for gaseous PN[76] represent the largest of which we are aware.[45] For N1 and N5, the three CSPVs are very different from one another, consistent with their encoding information emphasizing different orbitals and symmetry, and hinting at the value of knowing all three separately, for maximum insight into the electronics of the site (see for example references 40 and 77).

Ramsey's equation explains the large δ_{11} value of N5 (and N1) on the basis of the high-lying nonbonding electron pair that formally exists at both these sites. In contrast, N3 has three bonding partners (Figure 1), and its lone pair can be considered to participate in the π system instead of being nonbonding. Therefore, N3 is not expected to have such a strongly deshielded component, based on theory and the precedent of analogous N's in nucleoside bases.[47,77] Thus, the narrowest chemical shift tensor is entirely consistent with N3, as assigned, and the large spans of N5 and N1 are also consistent with their chemical natures.

For each of our flavin's three labeled N sites, the calculated isotropic average shift agrees extremely well with the observed isotropic shift (rmsd = 6 ppm, Table 1, Figure 6).[19] Individual calculated PVs agree less well with experiment (rmsd = 19 ppm), as has been found before.[36] Solvation effects can account for some of the discrepancies. The ^{15}N isotropic shift of pyridine in $CDCl_3$ is shielded by 12 ppm relative to the gas phase,[19,51,78] and this most likely represents predominantly effects on δ_{11}.[50,77,78] Therefore, a correction of −36 ppm to the calculated (gas phase) δ_{11} of N1 and N5 is likely justified and would bring these PVs within 9 and 15 ppm of experiment, respectively. This is also consistent with the findings of Grant and others that accounting for H-bonding significantly improves the accuracy of calculated chemical shifts,[48] from an rmsd of 37 to 14 ppm for ^{15}N in heterocycles.[47] With a −36 solvation ppm correction to δ_{11}, the calculated span of N5 becomes 731 ppm, close to the very large value obtained experimentally, and the rmsd between our experimental PVs and our calculated counterparts becomes 14 ppm. The computations also reproduce the narrower span of N1, which is discussed further below. Thus, the agreement between calculation and experiment validates the calculations, and the insights they can provide into flavin electronics.

^{13}C CSPVs were also measured, for natural abundance ^{13}C in lumiflavin, using 2d-PASS spectra at spinning speeds of 2.25 and 4 kHz. As anticipated, the aromatic C's were tightly clustered (Figure 7), as were two of the three methyls, and not all the anticipated signals could be resolved. Because the separation between clustered ^{13}C resonances was comparable to the variations in chemical shift observed upon changing the solvent or protein environment,[30,32] the powder sample's isotropic chemical shifts cannot be assigned by comparison with isotropic chemical shifts measured in solution, and selective labeling will be necessary in order to obtain reliable assignments, as has been found before.[79] Nonetheless, distinctive signals can be identified, such as the methyl C bound to N10, which has a chemical shift almost 10 ppm larger than those of the methyl C's bonded to C's C7 and C8,[79] and the signals of C9 and C4 with extreme isotropic shifts of 117 and 158 ppm, respectively. Adopting a best-case scenario in which observed signals were attributed to the calculated signals their PVs best matched, one

(73) Eichele, K.; Wasylishen, R. E. http://casgm3.anorg.chemie.uni-tuebingen.de/klaus/soft/index.html, 2005.
(74) Schweitzer, D.; Spiess, H. W. *J. Magn. Reson.* **1974**, *15*, 529−539.
(75) These data were acquired without the use of ^{1}H decoupling.
(76) Raymonda, J.; Klemperer, W. *J. Chem. Phys.* **1971**, *55*, 232−233.
(77) Stueber, D.; Grant, D. M. *J. Am. Chem. Soc.* **2002**, *124* (35), 10539−110551.
(78) Witanowski, M.; Sicinska, W.; Biernat, S.; Webb, G. A. *J. Magn. Reson.* **1991**, *91*, 289−300.
(79) Grande, H. J.; Gast, R.; van Schagen, C. G.; van Berkel, W. J. H.; Müller, F. *Helv. Chim. Acta* **1977**, *60* (2), 367−379.

is able to account extremely well for the resolved signals. Regression of the calculated values vs the best-matching resolved values produced a slope within experimental error of the theoretical value of 1.0 with relatively little scatter about the line ($R = 0.99$, Figure 7), and the rms difference between the CSPVs determined in the 2250 Hz-MAS 2d-PASS and the calculated sets of PVs that best match them was 10 ppm (6 ppm for isotropic values, Figure 7). Thus, these preliminary results bode well for the utility of ^{13}C CSPV's, but will require that signal assignments be made independent of the calculated values for the signals to serve as true measures of the quality of the calculation.

Relationships between ^{15}N Principal Chemical Shift Values and Molecular Orbitals. Because our ^{15}N signals are assigned based on experiment, independent of the calculations, these provide a stringent test of the calculations. Moreover, the ^{15}N signals are far easier to distinguish from one another than are the ^{13}C signals. The agreement between experimental and calculated ^{15}N principal chemical shift values validates other aspects of the calculations as well, including electronic properties relevant to reactivity, which are being pursued in more detail in further work. Here, we simply note that in systems dominated by paramagnetic shielding such as the N's of oxidized flavins, the calculated chemical shift eigenvectors' orientations in the molecular frame can reveal the symmetry of frontier orbitals, because the eigenvectors describe the directions about which electron density circulation occurs at the lowest energy cost (eq 1c). Thus, one eigenvector is perpendicular to the plane of the flavin rings for each of the N's. This is calculated to be δ_{33} for N1, N10, and N5 but δ_{22} for N3. In the case of N3, the experimental δ_{22} and δ_{33} values obtained from 1d CP-MASS spectra are not significantly different, so their identities with respect to the calculations may be interchanged. However, the values obtained from PASS spectra agree better with the calculation and indicate clearer separation of δ_{22} and δ_{33}. It therefore appears that N3's perpendicular deshielding may be slightly larger than the tangential deshielding, contrary to observations for several aromatic heterocycles[47] but consistent with results for several of the peptides for which tensors have been measured.[36,45] This suggests that N3 should not strictly be considered to be part of the aromatic π system.

Figure 8 depicts the calculated in-plane shielding eigenvectors of each of the nitrogens, in the molecular frame. As predicted by theory, and found for a series of heterocycles by Grant and others,[47] the tangential component is largest for N1 and N5, consistent with domination of this PV by terms involving the nonbonding lone pair.[51] For N10 and N3, the radial component is largest (and therefore named δ_{11}), also in agreement with theory and prior findings for substituted N's[47] (see supplemental Figure 1, Supporting Information).

The calculated radial eigenvectors of N10 and N3 both tilt clockwise in the presentation used for Figure 8. For N1 and N5, the radial eigenvectors are tilted clockwise too, but by much less. Consistent with the large tangential eigenvalues (Table 1), this more ideal calculated geometry likely also reflects the dominance of the lone pair, which tends to orient the tangential component orthogonal to itself (thus causing the radial eigenvector to be parallel with the lone pair). Thus, the δ_{11} calculated for N5 and N1 appear to strongly reflect the lone pair, and we can expect that experimental values will be sensitive to interactions of this orbital with H-bonding partners.

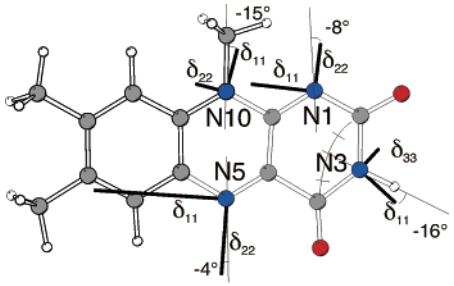

Figure 8. Oxidized flavin ring skeleton showing the orientations of calculated in-plane shielding eigenvectors, as solid straight lines. These are labeled according to the eigenvalue to which they correspond and the convention that the largest CSPV is named δ_{11}, the second largest δ_{22} and the smallest δ_{33}. The lengths of the solid lines are proportional to the magnitudes of the eigenvalues to which they correspond, as shown in Table 1. At all four N's, the remaining eigenvector is perpendicular to the molecular plane, and is not shown. Bonds of different order are not distinguished and the methyl group at N10 (top) reflects the fact that calculations were performed on lumiflavin. The light dashed lines depict the bisectors of the CNC angle at each N position (see N3) and are shown for the purpose of defining the angle between the radial eigenvector and the bisector, at each N position. O atoms are colored red, N atoms are blue, C atoms are gray, and H atoms are white.

The Bonding Changes Produced upon Reduction Are Readily Observed. Reduction of N5 converts this site from a "pyridine-type" N[80] to a N with a third bonding partner, in a less aromatic ring,[81] and therefore is predicted to make N5's signal much more similar to that of N3.[32] Indeed, reduction of dBF labeled only at N5 (to avoid confusion with the signal of N3) caused loss of the extremely anisotropic signal of N5 and its replacement by a much more isotropic signal at 50.4 ppm (Figure 9). Upon exposure to air, this signal disappeared and was gradually replaced by a highly anisotropic signal again. The chemical shift observed for the reduced flavin N5 is consistent with that of 59.4 ppm observed for reduced TARF in $CDCl_3$ [32] and the average of the calculated CSPVs, of $\delta_{iso} = 63.2$ ppm.[19] Individual CSPVs were calculated to be $\delta_{11} = 98.7$, $\delta_{22} = 56.7$, and $\delta_{33} = 34.1$ ppm, producing a span of 64.6 ppm, less than a tenth of that obtained for the same N site in the oxidized state. The calculated reduced-state span corresponds to a signal width of less than 2600 Hz at our field strength and thus is consistent with the absence of strong spinning sidebands at the MAS speed used (limited to > 2250 Hz by instability at lower speeds). Thus, not only the δ_{iso}[32] but also the CSPVs and span of the N5 SS−NMR signal are exceedingly sensitive to the changes in flavin electronics associated with redox activity, consistent with theory and DFT calculations.

Differences between the Oxidized Flavin N5 and N1 Chemical Shift Principal Values Correlate with the Elec-

(80) It has been common to refer to N1 and N5 of oxidized flavins as "pyridine-type" N's, whereas the N3 and N10 sites of oxidized flavins have been referred to as "pyrrole-type" N's refs 30 and 83. In the reduced state, all four N sites have been referred to as "pyrrole-type". We have retained the comparison between the N of pyridine and oxidized flavin's N1 and N5, as the δ_{11}s of both strongly reflect the nonbonded lone pair of the N and ring aromaticity. However, the decreased aromaticity of the reduced flavin system, as well as the different ring sizes, complicates comparison between the pyrrole N and the flavin N3 and N10, see ref 47. The issue of aromaticity has been addressed in detail in ref 81. Specifically, in the oxidized state, all three rings were found to be aromatic by the criteria of nucleus-independent chemical shifts, the anisotropy of the magnetic susceptibility, the unified Bird index, and natural bond orbital arguments (ref 81), supporting the possibility of comparing the oxidized flavin N1 and N5 with the N of pyridine, as a simple reference point.

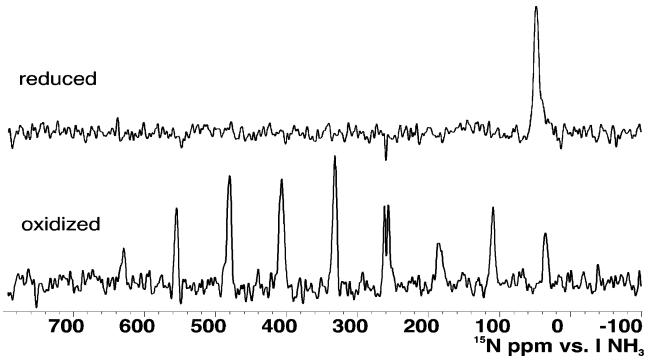

Figure 9. Effect of reduction on the N5 signal of [^{15}N−N5]-dBF. The signal of the reduced state (top) is compared with that of the oxidized state (below). For the oxidized state, 36 kHz ramped cross-polarization for 12 ms with MAS at 3 kHz were used at room temperature, with 60 s between scans (to minimize sample heating). For the reduced state, 36 kHz ramped cross-polarization was applied for a compromise duration of 8 ms with MAS at 3 kHz, at room temperature, with 30 s between scans. A center-band-glitch is evident in both spectra near 260 ppm.

trophilic vs Nucleophilic Reactivities of These Sites. The observed signal of N1 has a much smaller span than that of N5, with a much more shielded δ_{11} and significantly different δ_{22} and δ_{33} values as well, despite apparently similar local bonding. However, these differences agree with calculated differences. The differences are also consistent with N1 and N5's different chemistries. Among the 153 entries in Witanowski, Stefaniak, and Webb's compendium of pyridine-type ^{15}N signals, the isotropic shifts reported range from 215 to 333 ppm vs liquid ammonia.[82] In comparison, N5's isotropic shift of 345 ppm falls just above the high end, whereas N1's isotropic shift of 199 ppm is just below the low end. Thus, the flavin achieves very strong and opposite polarization of two pyridine-type N's that are only three bonds apart in a conjugated π system!

The highest chemical shifts listed by Witanowski et al. reflect pyridines with electron-withdrawing substituents *para* to the N, suggesting that N5's high chemical shift may be indicative of an electron density deficiency. This is entirely consistent with N5's electrophilic reactivity, as the site of sulfite modification and hydride acceptance from NAD(P)H.[83−85] In contrast, the low chemical shift end of the scale *tends* to reflect pyridines with electron donating groups.[82] Thus, N1's lower chemical shift is consistent with N1's more nucleophilic reactivity as the site of oxidized flavin protonation.[86] Both of these observations are consistent with calculated excess negative charge at N1.[87,88] Indeed, natural population analysis performed in conjunction with our chemical shift calculations produces charges equivalent to 0.62 of an excess electron (*e*) at N1 but only 0.34 *e* at N5. Some excess electron density is expected due to the greater electronegativity of N than the surrounding ring C's, but the almost 0.3 *e* greater excess electron density at N1 than at N5 is interesting and consistent with polarization of the flavin by the C═O functionalities of the uracyl ring.

Our calculated ^{13}C chemical shifts also make distinctions among superficially similar C sites with different reactivities. Moonen et al. have demonstrated strong polarization of the flavin by the carbonyl functionality at C2, especially in polar solvents that stabilize negative charge on O2a.[32] Thus, they rationalized deshielding of C8 relative to the superficially similar C7, consistent with our calculated isotropic chemical shifts of 151 ppm for C8 vs 138 ppm for C7. Moreover, the different shifts of C8 and C7 are associated with depletion of C8 by −0.04 *e* in contrast with a slight electron density excess of 0.03 *e* at C7, based on natural population analysis. Experimentally, the distinction between C8 and C7 increased in polar media as both sites shifted further downfield,[32] indicating that in-vacuuo calculations should be considered to be lower limits of any solution difference between the sites, and providing a rationale for the surprising susceptibility of the C8a methyl protons to exchange with solvent in aqueous solution.[89] These results suggest that calculations including solvation and specific noncovalent interactions will reveal greater differences between sites in the flavin, both with respect to natural charges and CSPVs.[90]

Concluding Remarks

We report the first characterization of the ^{15}N SS−NMR signals of oxidized flavin, demonstrating that distinct spectroscopic properties are observed for sites with distinct bonding and reactivity, consistent with theory, calculations and chemical precedent. Our observed and calculated chemical shift principal values are the first report of such for flavins, to our knowledge. Moreover, the current studies of free flavin will provide a useful baseline for additional studies aimed at understanding flavin reactivity in enzymes. The good agreement between observed and calculated chemical shift principal values validates the use of computation to interpret the ^{15}N SS−NMR signals of oxidized flavins in protein active sites and model systems. The changes observed upon reduction of N5 also agree well with those predicted by theory and calculations. It is gratifying to discover that not only the previously studied isotropic shifts[19,30−33] but even more so the very different chemical shift principal values measured here reflect extreme and distinct electronic properties for N5 and N1.

Enzyme cofactors give biological systems access to essential chemical reactivity that amino acids do not provide. The ^{15}N chemical shift principal values measured here for oxidized flavin are uniquely well suited to understanding flavin reactivity by virtue of their sensitivity to specific orbitals and, moreover, the very orbitals that dominate redox reactivity. We have proposed that ^{15}N chemical shift principal values can provide direct, orbital-, and atom-specific information related to fundamental determinants of flavin reactivity. This promises to be true (to a lesser extent) for ^{13}C as well. These principles should also be applicable to other important heterocyclic cofactors, such as pterins and pyridoxyl phosphate, suggesting that SS−NMR of labeled cofactors in proteins may prove a valuable tool for understanding enzyme catalysis at a fundamental level. We are

(81) Rodriguez-Otero, J.; Martinez-Nunez, E.; Pena-Gallego, A.; Vazquez, S. A. *J. O. C.* **2002**, *67*, 6347−6352.
(82) Witanowski, M.; Stefaniak, L.; Webb, G. A. *Nitrogen NMR Spectroscopy*. Academic Press: New York, 1981; Vol. 11B, p 1−493.
(83) Müller, F. *Chemistry and Biochemistry of Flavoenzymes.* CRC Press: Boca Raton, FL, 1991; Vol. 1.
(84) Shinkai, S.; Honda, N.; Ishikawa, Y.; Manabe, O. *J. Am. Chem. Soc.* **1985**, *107*, 6286−6292.
(85) Müller, F.; Massey, V. *J. Biol. Chem.* **1969**, *244*, 4007−4016.
(86) Sun, M.; Song, P.-S. *Biochemistry* **1973**, *12* (23), 4663−4669.
(87) Platenkamp, R. J.; Palmer, M. H.; Visser, A. J. W. G. *Eur. Biophys. J.* **1987**, *14*, 393−402.
(88) Hall, L. H.; Bowers, M. L.; Dufor, C. N. *Biochemistry* **1987**, *26*, 7401−7409.
(89) Bullock, F. J.; Jardetzky, O. *J. Org. Chem.* **1965**, *30*, 2056−2057.
(90) The important reactivity of the C4a site is manifest in the reduced state, which is not the focus of this work.

extending our SS−NMR studies to simple flavin complexes modeling interactions that tune the reactivity of flavins in proteins. Thus, we are developing the ability to understand ^{15}N SS−NMR signals of reactive positions in the flavin ring, in terms of the MOs that form the basis for flavin reactivity, and its tuning by proteins.[21,91]

Acknowledgment. We thank Mssrs. A. Sebesta and W. J. Layton of the University of Kentucky for assistance with NMR spectrometer upkeep, Dr. David Rice of Varian Inc. for generous technical advice, Dr. Eduard Checkmenev for early experiments, Bruce Lichtenstein of the University of Pennsylvania for assistance with syntheses, and Joe Clements, III, for help with the TOC graphic. R.L.K. acknowledges fellowship support under GM 64090, P.L.D. thanks the NIH for support under RO1 GM41048, R.J.W. thanks NIH for support under AR41751-07, and A.F.M. is grateful for NIH funding via R01 GM063921 and funding from the Petroleum Research Fund via PRF # 44321-AC4. The 400 MHz NMR spectrometer used was purchased thanks to funding from the National Science Foundation obtained under the MRI program Grant # DMR-9977388, and supercomputer access was obtained via allocation CHE020054 from the N.C.S.A. and courtesy of the C.S.S. of the University of Kentucky.

Supporting Information Available: A cartoon representation of the HOMO and LUMO that make major contributions to δ_{11} for a canonical "pyridine-type" N center with a nonbonding lone pair, and an analogous N center in which the radial in-plane orbital forms a bond with a substituent (Figure 1). Complete reference number 63. This material is available free of charge via the Internet at http://pubs.acs.org.

JA0648817

(91) Ghisla, S.; Massey, V. *Eur. J. Biochem.* **1989**, *181*, 1−17.